PROCEEDINGS OF SPIE

SPIEDigitalLibrary.org/conference-proceedings-of-spie

Supermode noise suppression in harmonically mode-locked fiber laser by continuous wave injection

Dmitry Korobko, Pavel Itrin, Valeria Ribenek, Dmitrii Stoliarov, Andrei Fotiadi

Dmitry A. Korobko, Pavel A. Itrin, Valeria Ribenek, Dmitrii Stoliarov, Andrei Fotiadi, "Supermode noise suppression in harmonically mode-locked fiber laser by continuous wave injection," Proc. SPIE 12142, Fiber Lasers and Glass Photonics: Materials through Applications III, 1214214 (25 May 2022); doi: 10.1117/12.2621025

SPIE.

Event: SPIE Photonics Europe, 2022, Strasbourg, France

Supermode noise suppression in harmonically mode-locked fiber laser by continuous wave injection

Dmitry A. Korobko*[a], Pavel A. Itrin[a], Valeria A. Ribenek[a], Dmitry A. Stoliarov[a] and Andrei A. Fotiadi[a, b, c]
[a]Ulyanovsk State University, L. Tolstoy str., 42, 432017, Ulyanovsk, Russia; [b]Ioffe Physical-Technical Institute, RAS, St. Petersburg 194021, Russia; [c] Electromagnetism and Telecommunication Department, University of Mons, Mons, B-7000, Belgium.

ABSTRACT

We report on suppression of supermode noise in harmonically mode-locked fiber laser achieved through the injection of continuous wave (CW) into the laser cavity. Implementing this method, we have shown experimentally that supermode suppression level of harmonically mode-locked laser could be increased by 20-30 dB depending on the pulse energy of the mode-locked laser. Experiments have refined the requirements to the positions inside the laser spectrum assigned to the injected CW component, a Kelly soliton sideband, and the transparency peaks of the birefringent filter formed in the ring fiber cavity. The effect takes places at proximity of the injected CW to the Kelly sideband leading to phase-locking between the CW and the solitons.

Keywords: fiber lasers, harmonic mode-locking, supermode noise suppression.

1. INTRODUCTION

Ultrafast mode-locked lasers with GHz repetition rates are of great interest in research and in technology, e.g., in optical telecommunications, frequency metrology, high-speed optical sampling, and data storage [1-4]. High beam quality, simplicity in adjustment, reliability, user-friendly light delivering make the fiber lasers an advantageous alternative to semiconductor and solid-state lasers [4-6]. Since the cavity length determines the fundamental repetition rate of the mode-locked lasers, it is impossible to have this value higher than tens to hundreds of MHz with the fiber lasers of standard length. To increase the pulse repetition rate of fiber lasers, a less technically challenging and more convenient way is the harmonic mode-locking (HML) scheme, where multiple pulses are evenly spaced in the cavity and the laser operates at a multiple of its fundamental frequency [2,3,7-15]. The HML could be implemented in the fiber laser cavity using a special intra-cavity periodic filter [2, 3, 8] or through active mode-locking procedure [9], however the most attractive way is the use of the passive harmonic mode-locking mechanism exploiting the pulse repulsion in the ring laser cavity [7, 11-13]. A wide range of passive HML laser configurations employing either real (SESAM, carbon nanotubes, etc) or artificial (nonlinear polarization rotation, etc) saturable absorbers have been demonstrated to operate with repetition rate up to tens of GHz [14-17].

The main drawback of the HML laser technology is the noise-induced irregularities of the time interval between the delivered pulses known as the HML timing jitter. Commonly, its value is significantly higher than the timing jitter of fundamentally mode-locked lasers [18, 19]. The HML timing jitter can be evaluated through the parameters of radiofrequency (RF) laser spectrum– that are the signal to noise ratio (S/N) and supermode suppression level (SSL), a specific HML laser characteristics [18]. Suppression of the supermode noise is a challenge of the HML laser technology directed to reduction of the timing jitter, widening the range of the HML laser applicability [19-26].

Here we propose a method of supermode noise suppression in HML lasers based on an external optical injection. In this method, a low-power signal from an external continuous-wave (CW) source is injected into the HML laser ring cavity. An effect of the externally injected CW on the pulse arrangement inside the passively HML laser cavity is still an essential point to be studied. On the one hand, the role of a CW background to act as an efficient interaction mediator between pulses has been advanced [27-29]. On the other hand it is reported that the HML regime remains unaffected by the injection of a tunable CW laser, whatever its wavelength, which tends to invalidate the positive influence of narrow CW component on the pulse-to-pulse stability [14]. The external CW injection has been used for increasing the SSL in the active HML laser based on the semiconductor optical amplifier [27]. Some experimental results on the enhancement

Fiber Lasers and Glass Photonics: Materials through Applications III, edited by Maurizio Ferrari,
Angela B. Seddon, Stefano Taccheo, Proc. of SPIE Vol. 12142, 1214214
© 2022 SPIE · 0277-786X · doi: 10.1117/12.2621025

of the HML stability in ring soliton fiber laser through the external CW injection have been demonstrated in [28, 29]. In this work we have improved understanding of this effect by exploring its specific properties. Our experimental results show that under certain conditions, the external CW injection into the cavity of the HML laser can significantly increase the SSL and promote the stability of harmonic pulse arrangement. We suggest that the nature of this effect is associated with the combined action of two main factors. The first is the interpulse repulsion that leads to automatic formation of periodic pulse pattern, and the second is phase locking between the CW and the solitons inducing the shift of the pulse carrier frequency. In a number of our previous works, the frequency shift has been shown to provoke an accelerated evolution of the perturbed HML system to an equilibrium point, improving the regularity of the harmonic pulse arrangement in the cavity [30-33]. This conclusion could be extrapolated to the laser configuration considered in this work, where the frequency shift is generated under the effect of the external CW.

2. EXPERIMENT

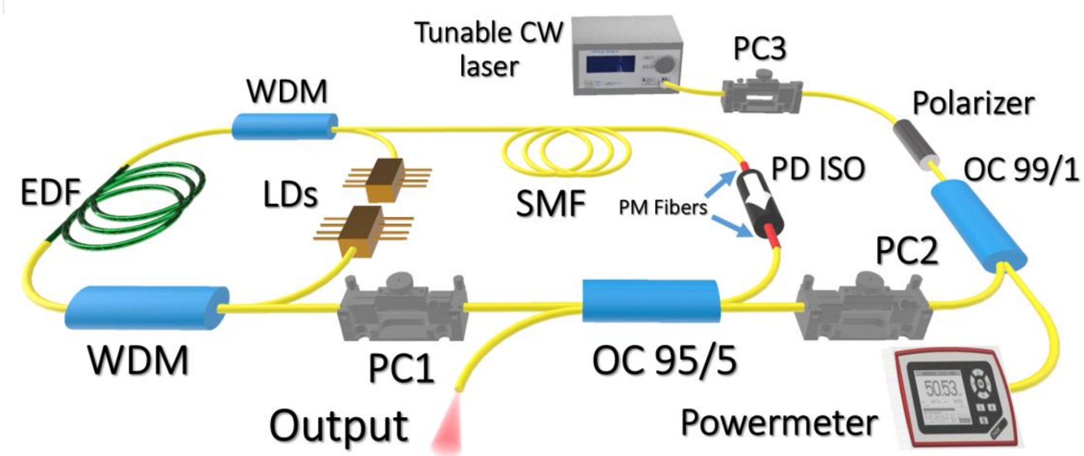

Fig. 1. Experimental setup. EDF – Er doped fiber, PC – polarization controller, PM ISO – polarization-maintaining isolator, OC – output coupler, LDs – laser pump diodes, WDMs – wavelength division multiplexors. Tunable CW laser is connected for supermode noise suppression.

We consider a standard configuration of the ring fiber laser mode-locked through the nonlinear polarization evolution (NPE). The laser setup is shown in Fig. 1. The cavity comprises a 0.8 m long heavily erbium-doped fiber (EDF 150), a polarization-maintaining (PM) fiber isolator with 0.7 m long PM fiber outputs, 980/1550 single mode WDM couplers, in-line polarization controller PC1 and 5% output coupler. The laser is pumped at 980 nm from laser diodes with the maximal power of 550 mW. The 20 m long laser cavity comprises three types of fibers: normal dispersion EDF (- 48 ps/nm /km), polarization-maintaining PM15-U25D (17.2 ps/nm/km) and standard anomalous dispersion single mode fiber (SMF-28) (18 ps/nm/km). The fundamental frequency of the ring fiber cavity is fT =14.1 MHz. The laser operation is monitored by an optical spectrum analyzer (HP 70950B) with resolution of 0.1 nm and radiofrequency spectrum analyzer (R&S FSP40) coupled with a 40 GHz photodetector (P40A Infrared & Microwave Technologies).

At a low pump power of about 50 mW a proper adjustment of the polarization state inside the cavity enables mode-locked laser operation at the fundamental frequency. The central wavelength of soliton laser operation can be tuned within some spectral regions due to a linear periodic-wavelength filter formed in birefringent fiber cavity [34]. We have found several such separate regions corresponding to certain settings of PC1 located in a wide range of wavelengths from 1550 to 1590 nm. Let us consider in more detail one of these regions located near the wavelength $\lambda \sim 1558$ nm. By increasing the pump, the laser operation switches to a multipulse generation. The HML with repetition rate multiple of the fundamental frequency can be implemented quite easily by careful adjusting the polarization controller PC1. Precise adjustment of the PC1 allows obtaining HML within this spectral area at the pulse repetition rate range of ~300 - ~3500 MHz, output power from 3.45 to 3.48 mW, and constant pump of about ~700 mW. The optical spectra of the obtained pulse trains highlight the expected feature – the repetition rate increases with the decrease of the single pulse energy which, in turn, causes a spectrum width narrowing. At higher single pulse energy the spectrum of the pulse train comprises the pronounced Kelly sidebands, but their amplitude rapidly decreases with an increase of the repetition rate. The laser's RF spectra features are typical for the HML lasers. The main peaks of the RF spectrum are spaced by the pulse repetition rate, whereas the surrounding supermode spurs are spaced by the fundamental frequency fT. The ratio of the highest peak intensity to the maximum intensity of surrounding supermode is the supermode noise suppression level (SSL), the main parameter determining the timing jitter and regularity of the pulse train generated by the HML laser [18].

In our experiment, the external frequency tunable CW laser (Yenista, module OSICS T100) has been connected to the ring fiber cavity through an output 5/95 coupler (Fig. 1). The CW laser line width is ~ 100 kHz. During the experiment, its output power is maintained at the level of about 3.5 mW. The laser polarization at the input to the cavity is controlled by PC2. Scanning the CW laser wavelength has shown that strong perturbations of the fiber laser optical and RF spectra resulted from interaction between the solitons and injected CW arise only at the wavelength of the external laser lying within periodically spaced narrow bands around the wavelengths λ ~ 1544nm, 1555nm, 1566nm, 1577nm. We identify these bands as the peaks of the periodic wavelength filter [34]. Having the external laser wavelength fixed within one of the bands near λ ~ 1566 nm, we observe the HML achieved at the central pulse wavelength within the band near λ ~ 1558 nm considered earlier. Same as before we get the pulse trains with repetition rates ~300 - ~3500 MHz obtained at constant pump of about ~700 mW. By careful adjusting PC1, we can shift the position of the soliton optical spectrum in respect to the wavelength of external laser. Analyzing the changes in the optical and RF spectra at different relative positions of the broadband soliton spectrum and the external laser we could evaluate the efficiency of the interaction between the soliton and CW. Our observations have shown that the optical and RF spectra of the pulse train almost do not change when the CW is far from the top of the soliton optical spectrum. On the contrary, when the CW is close to the soliton spectrum maximum, the laser most often stops its HML operation and the pulse train decay occurs.

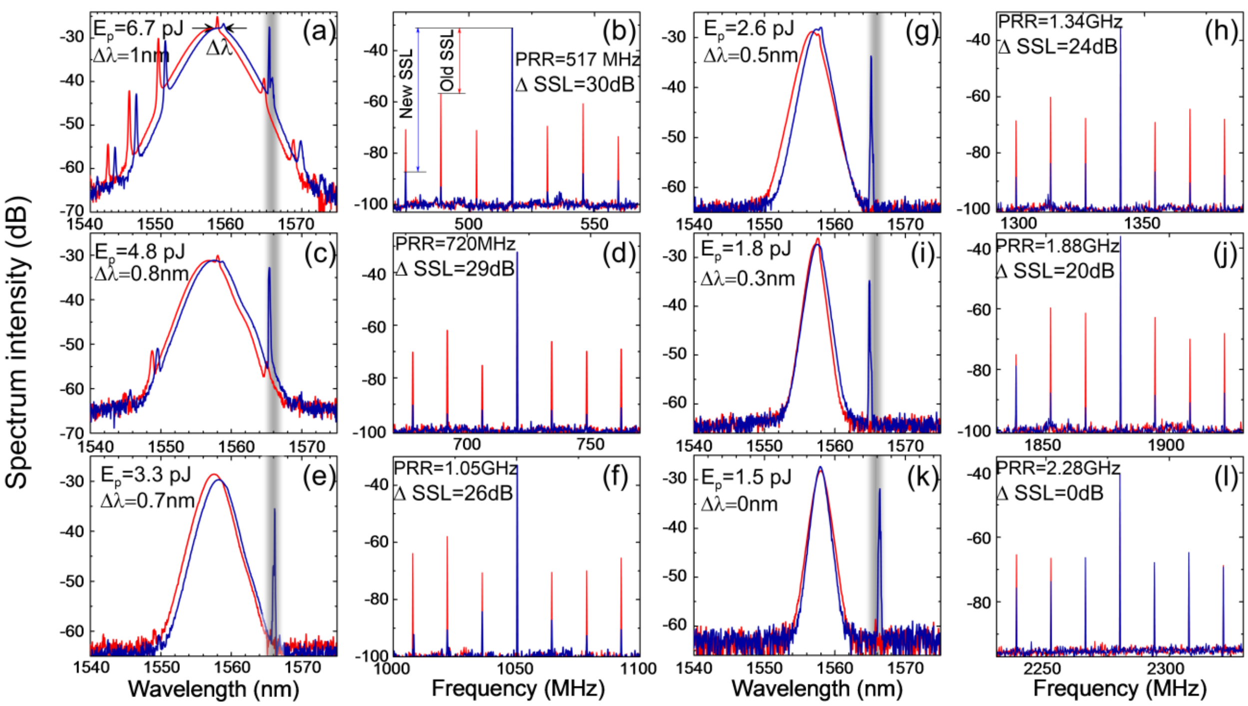

Fig. 2. Optical and RF spectra recorded with the HML fiber laser before (red curve) and after (blue curve) the CW light injection at different PRR. The single soliton energy , optical spectrum shift , SSL difference before and after the CW injection , PRR are also depicted. RF spectra have been obtained in a 100 MHz span with a 200 kHz resolution. The only FTM band in the presented spectrum range is marked (grey).

Let us consider this interaction when the CW lies within a certain range between the soliton spectrum top and pedestal. It is found that when the pronounced first-order Kelly sideband in the spectrum of the pulse train with a repetition rate of 517 MHz approaches the CW, the level of supermode noise in the RF spectrum drops down, i.e. the SSL increases. Additional adjustment of the PC2 enables the SSL increase of 30 dB – from the initial level of 25 dB (before the CW injection) up to 55 dB (Fig 2 (a, b)). Importantly, the SSL growth is accompanied by the shift of the soliton optical spectrum by 1 nm towards the CW.

Similar effects have been found for the pulse trains with higher repetition rates (Fig. 2 (c-j)). As mentioned above, the single pulse energy and the spectrum width decrease with an increase of the repetition rate. The Kelly sidebands, observed in the optical spectrum at the repetition rate of f = 720 MHz, are no longer registered at the higher frequencies and lower pulse energies. However, an increase of the SSL is still observed in these cases. One should note that in all these cases, the spectral distance between the pulse spectrum maximum and the injected CW remains almost constant. It is known that the spectral position of the Kelly sidebands exhibits a weak dependence on the pulse energy, but their intensity rapidly decreases with the pulse energy decrease [34]. Thus, we can conclude that even in the case when the Kelly sidebands are hardly recognizable, the CW has to be spectrally close to them to provide an increase of the SSL. Our experimental results show that the SSL growth reduces when the single pulse energy and wavelength shift of the spectrum decrease. For the repetition rates f > 2000 MHz and pulse energies <1.7 pJ, no significant increase in the SSL has been achieved (Fig. 2 (k, l)) highlighting the negligible interaction between the solitons and CW at low single pulse energies.

The RF spectra discussed above were obtained near the main RF peak corresponding to the pulse repetition rate. Now, let us consider the large-scaled RF spectra extended for the range of several harmonics of the repetition rate (Fig. 3). The Figs. 3 (a, c) and (b, d) show the extended RF spectra of the pulse train with the repletion rate of 517 MHz and 1880 MHz, corresponding to the Figs. 2 (a, b) and Figs. 2 (i, j) respectively. Noteworthy, in both cases, a drastic decrease of the supermode noise level is observed after the CW injection.

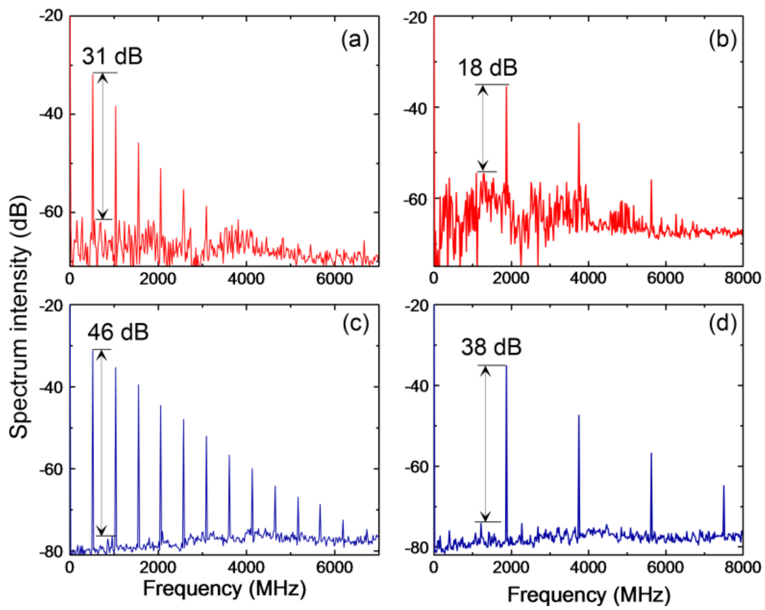

Fig.3. RF spectra with a resolution bandwidth of 20 MHz for pulse trains with repetition rates (a, c) f = 517 MHz, (b, d) f = 1880 MHz. Figs. (a, b) show the spectra before the CW injection, (c, d) after the CW injection.

As mentioned above, the essential changes in the RF spectrum of the HML pulse train occur only when the CW is injected into the one of the periodically located narrow bands corresponding to the transmission peak of the ring fiber cavity. Fig. 4 shows the optical spectra of pulse trains with the same repetition rate f = 517 MHz with observed increase in the SSL after the CW injection. The spectral period of these injection bands is approximately 11 nm. This period is well consistent with the spectral period corresponding to the linear transmittance of a 20 m low-birefringent ring fiber cavity including the short segment of PM fiber. Fig. 4 shows that the SSL increase can be observed only if the CW is located in close proximity to the one of the Kelly sidebands of pulse train optical spectrum. The experiment shows that the maximum increase of the SSL (about 30 dB) is observed when the CW is close to the first-order Kelly sideband (spectra # 3, 4, 5). In these cases, the maximum wavelength shift $\Delta\lambda \approx 1$ nm is also observed. The CW interaction with the solitons in the region of the second (spectrum #1) or third order (spectrum #2) Kelly sideband is of lower intensity leading to smaller wavelength shift ($\Delta\lambda \approx 0.5$ nm for spectrum #1 and $\Delta\lambda \approx 0.3$ nm for spectrum #2) and smaller increase of the SSL (about 25 dB for spectrum #1 and 20 dB for spectrum #2).

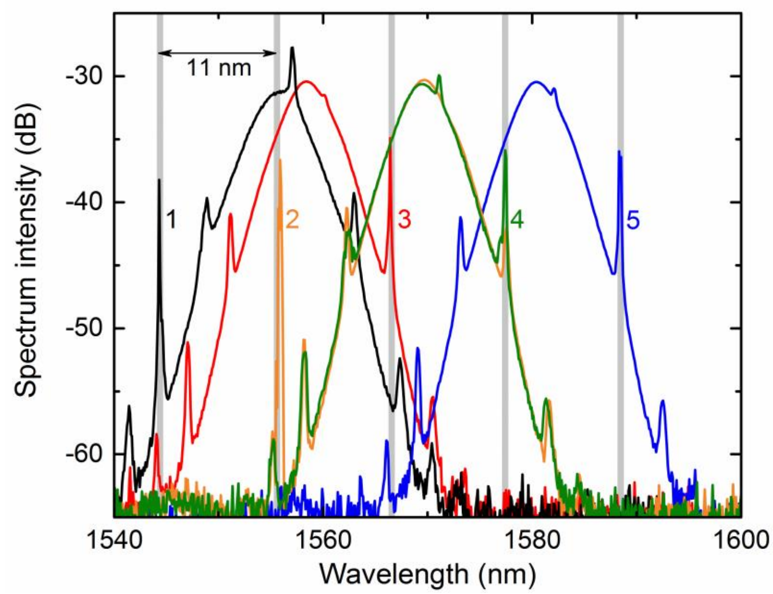

Fig. 4. Optical spectra of pulse trains with observed increase of the SSL after the CW injection. The repetition rate is 517 MHz. The spectra are shown with the reference to the CW injection band around wavelength λ_{cw}. Spectrum 1 (black line) – $\lambda_{cw} = 1544$ nm, 2 (orange) – $\lambda_{cw} = 1555$ nm, 3 (red) – $\lambda_{cw} = 1566$ nm, 4 (green) – $\lambda_{cw} = 1577$ nm, 5 (blue) – $\lambda_{cw} = 1588$ nm.

3. DISCUSSION AND CONCLUSION

The integral timing jitter of the pulse train can be obtained from the relation

$$\Delta t = \frac{1}{2\pi f_N}\sqrt{\int L(f)df} \, ,$$

where f_N is the pulse repetition rate and L is the spectral density of the phase noise. High supermode noise provokes a drastic increase of the timing jitter in the HML lasers compared to the lasers operating fundamental mode-locking, since the jitter shows steplike increase at each supermode spur while integrating over the frequencies $f \geq f_T$. With the SSL increasing by 20-30 dB, the timing jitter of the HML pulse train can be reduced by almost an order of magnitude [27].

The resonant interaction between the CW and soliton, which takes place when the CW component is close to one of the Kelly sidebands underlies the physics of the observed effect. It is well known that soliton circulating in fiber cavity undergoes periodical disturbances, which couple the soliton to the co-propagating low amplitude radiation (so-called dispersion waves). The phase difference between the soliton and dispersion waves is constant and multiple of 2π [35]. Injection of the external CW at the wavelength close to the wavelength of dispersive waves, i.e. to the Kelly sideband leads to phase locking of the soliton and CW [36]. The phase difference for any two points of the united field is constant and the united structure moves as a whole. As a result, the carrier frequency of the soliton is shifted and the value of the shift is determined by the parameters of the soliton and injected CW. In our previous works [30-33], we have shown that the shift of the carrier frequency from the center of the spectral filter could improve the HML regularity suppressing the supermode noise and reducing the timing jitter of the HML fiber ring laser. Physically, this effect is associated with the accelerated evolution of the frequency shifted system to the equilibrium point corresponding to harmonic distribution of the pulses in the cavity that is equivalent to increasing in interpulse repulsion [11].

In the considered configuration, the filter is provided by a combined action of the laser gain line and transmission bands of the birefringent ring cavity. The carrier frequency shift occurs through phase locking of the soliton and CW. The CW induced frequency shift leads to stabilization of the harmonic pulse distribution and decrease of supermode noise. However, the stabilization effect is reduced at a lower frequency shift. Finally, when the pulse energy is below a certain value, the intensity of the resonant interaction drops to a negligible level and the effect of the SSL increase vanishes.

We have shown that the SSL increase is observed in a wide spectrum range. This effect occurs only when the CW coincides with the peaks of the periodic wavelength filter (Fig. 4). On the other hand, the pulse spectrum position is bounded by two spectral ranges of successful HML determined not only by this filter, but also by the spectrum offset from the gain spectrum peak. As a result, in some cases, the CW could be adjusted to a low-intensity high-order Kelly peak only, e.g., the second-order peak of spectrum #1 and the third-order peak of spectrum # 2 (Fig. 4). In these cases, the frequency shift and the SSL increase are also observed despite rather weak interaction between the CW and soliton.

Summarizing, in our experiment we have observed the effect of supermode noise suppression in the ring fiber soliton HML laser implemented through the external CW injection. This effect takes places at proximity of the injected CW to the Kelly sideband of soliton spectrum leading to phase locking between the CW and the solitons. The soliton frequency shift arising due to phase locking ensures the accelerated evolution of the system to the equilibrium point and makes the arrangement of pulses in the cavity more regular. The proposed supermode noise suppression technique can be applied to reduce the timing jitter of the HML fiber laser down to a level comparable to the jitter of the lasers operating fundamental mode-locking, thus making the HML lasers promising for many applications.

This work was supported by the Russian Science Foundation (19-72-10037) and the Russian Ministry of Higher Education and Science (project 075-15-2021-581). P.A.I. is partially supported by the RFBR (20-32-90171).

REFERENCES

[1] Diddams, S. A., Vahala, K. and Udem, T., "Optical frequency combs: Coherently uniting the electromagnetic spectrum," Science 369, 6501 (2020).

[2] Peccianti, M., Pasquazi, A., Park, Y., Little, B. E., Chu, S. T., Moss, D. J. and Morandotti, R., Demonstration of a stable ultrafast laser based on a nonlinear microcavity. Nature communications 3(1), 1-6 (2012).

[3] Mao, D., Liu, X., Sun, Z., Lu, H., Han, D., Wang, G. and Wang, F., "Flexible high-repetition-rate ultrafast fiber laser," Scientific reports 3(1), 1-5 (2013).

[4] Gumenyuk, R., Okhotnikova, E. O., Filippov, V., Korobko, D. A., Zolotovskii, I. O. and Guina, M., "Fiber lasers of Prof. Okhotnikov: review of the main achievements and breakthrough technologies," IEEE Journal of Selected Topics in Quantum Electronics 24(3), 1-14 (2017).

[5] Rissanen, J., Korobko, D. A., Zolotovsky, I. O., Melkumov, M., Khopin, V. F. and Gumenyuk, R., "Infiltrated bunch of solitons in Bi-doped frequency-shifted feedback fibre laser operated at 1450 nm," Scientific reports 7(1), 1-10 (2017).

[6] Aleshkina, S. S., Fedotov, A., Korobko, D., Stoliarov, D., Lipatov, D. S., Velmiskin, V. V.and Likhachev, M. E., "All-fiber polarization-maintaining mode-locked laser operated at 980 nm," Optics letters 45(8), 2275-2278 (2020).

[7] Liu, X. and Pang, M., "Revealing the buildup dynamics of harmonic mode-locking states in ultrafast lasers," Laser & Photonics Reviews 13(9), 1800333 (2019).

[8] Korobko, D.A., Fotiadi, A.A., Zolotovskii, I.O., "Mode-locking evolution in ring fiber lasers with tunable repetition rate," Optics Express 25(18), 21180-21190 (2017).

[9] Wang, Y., Set, S. Y., Yamashita, S., "Active mode-locking via pump modulation in a Tm-doped fiber laser," APL Photonics 1(7), 071303 (2016).

[10] Cheng, H., Wang, W., Zhou, Y., Qiao, T., Lin, W., Guo, Y., Yang, Z., "High-repetition-rate ultrafast fiber lasers," Optics Express 26(13), 16411-16421 (2018).

[11] Kutz, J. N., Collings, B. C., Bergman, K., Knox, W. H., "Stabilized pulse spacing in soliton lasers due to gain depletion and recovery," IEEE Journal of Quantum Electronics 34(9), 1749-1757 (1998).

[12] Kbashi, H. J., Sergeyev, S. V., Al-Araimi, M., Rozhin, A., Korobko, D. and Fotiadi, A., "High-frequency vector harmonic mode locking driven by acoustic resonances," Optics Letters 44(21), 5112-5115 (2019).

[13] Ribenek, V. A., Stoliarov, D. A., Korobko, D. A. and Fotiadi, A. A., "Pulse repetition rate tuning of a harmonically mode-locked ring fiber laser using resonant optical injection," Optics Letters 46(22), 5687-5690 (2021).

[14] Lecaplain, C., Grelu, P., "Multi-gigahertz repetition-rate-selectable passive harmonic mode locking of a fiber laser," Optics Express 21(9), 10897-10902 (2013).

[15] Stoliarov, D. A., Itrin, P. A., Ribenek, V. A., Korobko, D. A. and Fotiadi, A. A., "Linear cavity fiber laser harmonically mode-locked with SESAM," Laser Physics Letters 17(10), 105102 (2020).

[16] Stoliarov, D. A., Itrin, P. A., Korobko, D. A., Ribenek, V. A., Tabulina, L. V., Sysa, A. V. and Shaman, Y. P., "Saturable absorber based on the fiber coupler coated by CNTs," Optical Fiber Technology 63, 102524 (2021).
[17] Zolotovskii, I. O., Korobko, D. A., Gumenyuk, R. V. and Okhotnikov, O. G., "Generation of bound states of pulses in a soliton laser with complex relaxation of a saturable absorber," Quantum Electronics 45(1), 26 (2015).
[18] Rana, F., Lee, H. L., Ram, R. J., Grein, M. E., Jiang, L. A., Ippen, E. P. and Haus, H. A., "Characterization of the noise and correlations in harmonically mode-locked lasers," JOSA B 19(11), 2609-2621 (2002).
[19] Gumenyuk, R. V., Korobko, D. A., Zolotovskii, I. O., "Stabilization of passive harmonic mode locking in a fiber ring laser," Optics Letters 45(1), 184-187 (2020).
[20] Nakazawa, M., Tamura, K. and Yoshida, E. "Supermode noise suppression in a harmonically modelocked fibre laser by self-phase modulation and spectral filtering," Electron. Lett. 32, 461–463 (1996).
[21] Pottiez, O., Deparis, O., Kiyan, R., Haelterman, M., Emplit, P., Mégret P., and M. Blondel, "Supermode noise of harmonically mode-locked erbium fiber lasers with composite cavity," IEEE journal of quantum electronics 38, 252-259 (2002).
[22] Schröder, P., Alasia, D., Sylvestre, T., and Coen, S., "Dynamics of an ultrahigh-repetition-rate passively mode-locked Raman fiber laser," JOSA B 25, 1178-1186 (2008).
[23] Yuhua, L., Caiyun, L., Jian, W., Boyu, W. and Yizhi, G., "Novel method to simultaneously compress pulses and suppress supermode noise in actively mode-locked fiber ring laser," IEEE Photon. Technol. Lett. 10, 1250–1252 (1998).
[24] Lin, G.-R., Wu, M.-C. and Chang, Y.-C. "Suppression of phase and supermode noise in a harmonic mode-locked erbium-doped fiber laser with a semiconductor-optical- amplifier-based high-pass filter," Optics Letters 30, 1834–1836 (2005).
[25] .Zolotovskii, I. O., Korobko, D. A. and Lapin, V. A., "Modulation instability and short-pulse generation in media with relaxing Kerr nonlinearity and high self-steepening," Quantum Electronics 44(1), 42(2014).
[26] Korobko, D. A., Zolotovskii, I. O., Svetukhin, V. V., Zhukov, A. V., Fomin, A. N., Borisova, C. V. and Fotiadi, A. A., "Detuning effects in Brillouin ring microresonator laser," Optics Express 28(4), 4962-4972 (2020).
[27] Quinlan, F., Gee, S., Ozharar, S. And Delfyett, P. J., "Greater than 20-dB supermode noise suppression and timing jitter reduction via CW injection of a harmonically mode-locked laser," IEEE Photonics Technology Letters 19(16), 1221-1223 (2007).
[28] Niang, A., Amrani, F., Salhi, M., Leblond, H., Komarov, A. and Sanchez, F., "Harmonic mode-locking in a fiber laser through continuous external optical injection," Optics Communications 312, 1-6 (2014).
[29] Semaan, G., Komarov, A., Salhi, M., Sanchez, F., "Study of a harmonic mode lock stability under external continuous-wave injection," Optics Communications 387, 65-69 (2017).
[30] Korobko, D. A., Stoliarov, D. A., Itrin, P. A., Ribenek, V. A., Odnoblyudov, M. A., Petrov, A. B., Gumenyuk, R. V., "Stabilization of a Harmonic Mode-Locking by Shifting the Carrier Frequency," Journal of Lightwave Technology 39(9), 2980-2987 (2021).
[31] Korobko, D. A., Stoliarov, D. A., Itrin, P. A., Odnoblyudov, M. A., Petrov, A. B., Gumenyuk, R. V., "Harmonic mode-locking fiber ring laser with a pulse repetition rate up to 12 GHz," Optics & Laser Technology 133, 106526 (2021).
[32] Ribenek, V. A., Stoliarov, D. A., Korobko, D. A. and Fotiadi, A. A., "Mitigation of the supermode noise in a harmonically mode-locked ring fiber laser using optical injection," Optics Letters 46(22), 5747-5750 (2021).
[33] Liu, X., Närhi, M., Korobko, D.and Gumenyuk, R., "Amplifier similariton fiber laser with a hybrid-mode-locking technique," Optics Express 29(22), 34977-34985 (2021).
[34] Chen, C. J., Wai, P. K. A. and Menyuk, C. R., "Soliton fiber ring laser," Optics letters 17(6), 417-419 (1992).
[35] Dennis, M. L. and Duling, I. N., "Experimental study of sideband generation in femtosecond fiber lasers," IEEE Journal of Quantum electronics 30(6), 1469-1477 (1994).
[36] Komarov, A., Komarov, K., Niang, A., Sanchez, F., "Nature of soliton interaction in fiber lasers with continuous external optical injection," Physical Review A 89(1), 013833 (2014).